Deep-Sea Research I 57 (2010) 65–77

Contents lists available at ScienceDirect

Deep-Sea Research I

journal homepage: www.elsevier.com/locate/dsri

Trichodesmium spp. population structure in the eastern North Atlantic subtropical gyre

Fernando González Taboada *, Ricardo González Gil, Juan Höfer, Sonia González, Ricardo Anadón

Área de Ecología. Dpto. Biología de Organismos y Sistemas de la Universidad de Oviedo, C/ Valentín Andrés Álvarez s/n, E33071, Oviedo, Asturias, España

ARTICLE INFO

Article history:
Received 27 March 2009
Received in revised form
12 September 2009
Accepted 25 September 2009
Available online 4 October 2009

Keywords:
Diazotroph
Nitrogen cycle
Size structure
North Atlantic subtropical gyre
Trichodesmium

ABSTRACT

Trichodesmium spp. population structure was studied based on a transect in the eastern subtropical North Atlantic in October 2006, covering a gradient from near-temperate conditions up to fully subtropical, oligotrophic waters. *Trichodesmium* spp. trichomes were counted and measured, distinguishing free trichomes from those forming macroscopic colonies (“puffs” or “tufts”). Moreover, for both free and colonial individuals, abundance and size structure variation were quantified from single trichome-level data. Nitrogen fixation rates were estimated using an empirical approach based on abundance observations and a heuristic approach to incorporate variation in trichome size and environmental temperature. A gradual change towards greater sizes and increased abundances was observed as physical conditions became subtropical. An extreme response was detected at one station (29.8°W, 26.3°N), in which both *in situ* and remote sensing data revealed the presence of a *Trichodesmium* bloom. Despite the presence of a mesoscale anticyclonic eddy, a close examination of prior surface conditions using altimeter data indicated that the bloom was related to the advection of southern waters. In general, our results highlighted the importance of free trichomes in *Trichodesmium* spp. populations in this part of the North Atlantic. Furthermore, they suggested a possible role of both size and population structure on the wide range of N_2 fixation estimates currently available in the literature.

1. Introduction

The role of species from the genus *Trichodesmium* in the nitrogen cycle remains one important objective of climate change research, given that they account for 25–50% of nitrogen fixation in the world's oceans (Capone et al., 1997; Karl et al., 2002; Mahaffey et al., 2005). Indeed, its extent and importance is an issue of continued debate, especially for the North Atlantic basin (Capone et al., 2005; Montoya et al., 2007; Deutsch et al., 2007; Reynolds et al., 2007). Because of their potential to fix atmospheric N_2, these buoyant species play an important role in the patterns of marine primary productivity in tropical and subtropical zones around the globe (Capone et al., 1997; Wilson and Qiu, 2008). They are also important in processes relevant to other global biogeochemical cycles, such as the regulation of ocean/atmosphere CO_2 balances (Falkowski, 1997; Gruber, 2004).

Thichodesmium spp. (hereafter, *Trichodesmium*) ability to fix N_2 has the cost of the high energetic demands associated with the nitrogenase activity. These costs are surpassed to some extent through buoyancy regulation and the development of photosystems that are efficient at high light conditions. N_2 fixation is limited mainly by the availability of phosphorus and iron (Berman-Frank et al., 2001; Sañudo-Wilhelmy et al., 2001; Mills et al., 2004). Deep-water intrusion is the main source of inorganic phosphorus in the subtropical ocean (Williams and Follows, 2003), although because of the permanent stratification, regenerated forms are more important for plankton. Indeed, *Trichodesmium* presents a great ability to cleave and take up dissolved organic phosphorus (Sohm and Capone, 2006). Aeolian dust deposition is considered as the main source of iron (Mills et al., 2004; Mahowald et al., 2009), a process that is especially important in the North Atlantic (Gao et al., 2001). Nevertheless, it has been recently proposed that spatial variation in N_2 fixation simply mirrors and balances changes in denitrification rates (Deutsch et al., 2007). Elevated seawater temperatures also favour *Trichodesmium* because nitrogenase activity is ineffective bellow 20 °C (Capone et al., 1997; Breitbarth et al., 2007). Other processes promoting *Trichodesmium* growth are reduced vertical mixing and anticyclonic eddies (Capone et al., 1997; Davis and McGillicuddy, 2006; McGillicuddy et al., 2007).

These cyanobacteria present a unique set of physiological and morphological adaptations for life under the severe conditions of tropical and subtropical oceans. These adaptations allow them to persist and become an abundant phytoplankton group, mainly

* Corresponding author. Tel.: +34 985 104794; fax: +34 985 104777.
E-mail address: fgtaboada@gmail.com (F. González Taboada).

0967-0637/$ - see front matter © 2009 Elsevier Ltd. All rights reserved.
doi:10.1016/j.dsr.2009.09.005

because nitrogen availability in these environments is extremely low. At the same time, they serve as physical substratum and food source for a diverse array of organisms (Paerl et al., 1989; O'Neil and Roman, 1992), mainly bacteria, which through regeneration can further funnel *Trichodesmium* production to other components of the food chain (Sellner, 1992). These characteristics define *Trichodesmium* as a key species in the warm, oligotrophic regions of the world ocean (Capone et al., 1997). Much of the existing literature on this group of species has focused on how different environmental factors influence N_2 fixation rates (Capone et al., 1997; Bhat and Verlecar, 2006). This effort resulted in a wide, overlapping range of N_2 fixation rates for different species and morphotypes (Orcutt et al., 2001; Karl et al., 2002; Carpenter et al., 2004; Capone et al., 2005; Mahaffey et al., 2005).

One of the characteristics less explored is the wide variation in population structure that these species present in the ocean. Most often, studies have considered only two of the macroscopic colonial forms, i.e. "tufts" (fusiform colonies) and "puffs" (spherical ones), although there is a third component usually present and commonly ignored. This is composed of free trichomes, single filaments of attached cells that can arrange themselves either in parallel or radially to form tufts or puffs, and that also present the ability to fix N_2. Individual free trichomes also show the highest growth rates under laboratory conditions (Saino and Hattori, 1982; Ohki and Fujita, 1988), and their dominance is thus assumed to indicate an active dynamic state in *Trichodesmium* populations.

Previous work conducted at station ALOHA (central, subtropical North Pacific) by Letelier and Karl (1996, 1998) and at the BATS site (western subtropical North Atlantic) by Orcutt et al. (2001) has shown that free trichomes could represent an important fraction of *Trichodesmium* populations, contributing up to 75% of *Trichodesmium* N_2 fixation (Orcutt et al., 2001). This figure makes desirable, if not unavoidable, the inclusion of such a component in *Trichodesmium* studies, although the bias towards focusing only on colonies is still present and remains apparently neglected in the recent literature. The work of Orcutt et al. (2001) also highlighted the importance of colony size in determining N_2 fixation rates, as did more recent work by Goebel et al. (2007) working at the ALOHA time-series station.

In the eastern North Atlantic, good coverage of some of these issues has been provided by the basin-scale study of Carpenter et al. (2004), although data was available only for tropical latitudes on the eastern side of the ocean. Tyrrell et al. (2003) summarized *Trichodesmium* abundance data retrieved during the AMT programme, but their samples were restricted to the east of ~20°W. Finally, Davis and McGillicuddy (2006) presented nearly continuous abundance estimates for the northern limit of this zone, although they ignored free trichomes. This leaves an empty region encompassing the eastern subtropical North Atlantic in the data used in almost all the subsequent direct modelling efforts (e.g. Hood et al., 2004; Montoya et al., 2007), despite the fact that it is within the *Trichodesmium* distributional range. Remote sensing data suggest that *Trichodesmium* blooms are frequent only during autumn in this region (Westberry and Siegel, 2006; Wilson and Qiu, 2008). Also, the modelling study by Reynolds et al. (2007) inferred that N_2 fixation rates are not especially high. The same was found by Deutsch et al. (2007), although they also concluded that the fraction of the export flux represented by fixed N_2 is important.

Here, we present *Trichodesmium* abundance data derived from samples retrieved along a transect in the eastern subtropical North Atlantic as part of the CARPOS cruise (*Plankton CARbon fluxes in Subtropical Oligotrophic environments: a lagrangian approach*). Relevant environmental factors were studied using both *in situ* and remote sensing data, including bloom detection algorithms. Abundance and size measurements of both single trichomes and colonial forms were used to describe population patterns of variation in abundance and size. Finally, variation in N_2 fixation rates in this region of the North Atlantic was explored, including the potential influence of changes in population structure.

2. Materials and methods

During the CARPOS cruise (October–December, 2006), aboard R.V. "Hespérides", eight stations were sampled (E0, October 14, 2006, 13.9°W 34.1°N; to E7, October 21, 2006, 36.7°W 25.4°N) encompassing the transition from nearly temperate to fully subtropical, oligotrophic conditions (Fig. 1). At each station, after

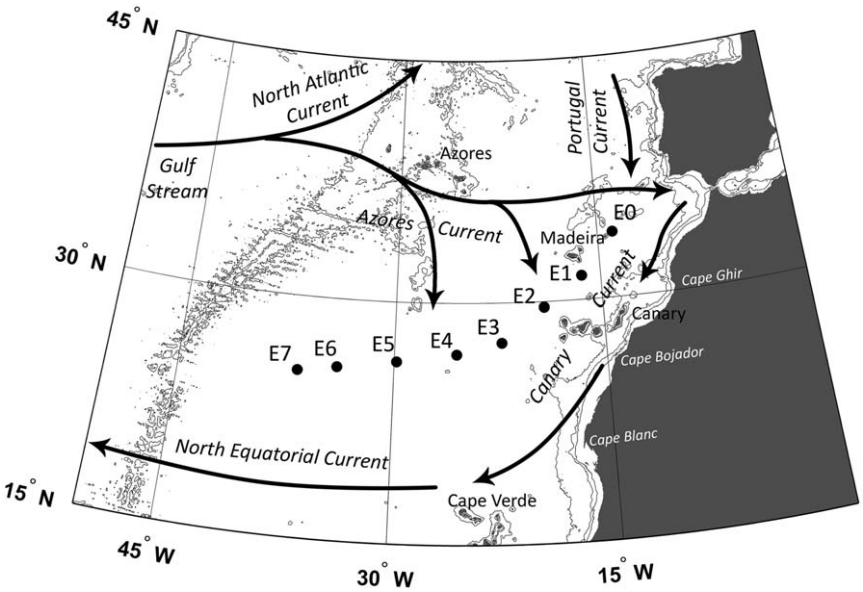

Fig. 1. Map of transect design showing the main oceanographic features of the study area.

characterization of the physical and chemical conditions of the water-column, *Trichodesmium* populations were sampled using vertically towed nets. Finally, we complemented our field data with remote sensing images to recover large-scale surface conditions in both physical and biological variables, including an algorithm designed to detect *Trichodesmium* blooms.

2.1. Area of study

Circulation in the eastern subtropical North Atlantic is characterized by weak flows and, in contrast to the western part, is not dominated by well-defined, narrow currents (Tomczak and Godfrey, 2001). Longhurst (2007) identifies two main regions: the North East Atlantic Subtropical Gyre Province (NASTE) in the west, and the Canary Coastal Province (CNRY) between the gyre and Africa. Changes in westerlies and trade wind forcing from spring to winter promote a seasonal cycle of expansion and contraction of NASTE, which has an inverse effect on the extent of CNRY (Stramma and Siedler, 1988; McClain et al., 2004).

The NASTE is bounded on the north by the Azores front and on the northeast by the southern branch of the Azores Current (Käse and Siedler, 1982; Klein and Siedler, 1989). This current supplies the Canary Current, which forms the eastern and southeastern boundaries of the gyre. The Canary Current is the major feature of CNRY and flows southward between 30°N and 10°N. This is the eastern boundary current associated with permanent coastal upwelling along the northwest African coast (Mittelstaedt 1991). The Canary Current then joins the North Atlantic Equatorial Current to close the gyre, establishing the southeastern limit of the NASTE (Fig. 1, Siedler and Onken, 1996).

Mesoscale features are frequent at all these fronts (Käse and Siedler, 1982; Barton et al., 1998; Johnson and Stevens, 2000), although their impact in primary production remains controversial in this low-energy region (Oschlies, 2002; McGillicuddy et al., 2003; Pingree, 1996; Pingree and García-Soto, 2004; Mouriño et al., 2005; McGillicuddy et al., 2007). Another important source of nutrients is aeolian dust deposition (Gao et al., 2001; Mills et al., 2004; Neuer et al., 2004; Mahowald et al., 2009), given the proximity of the Sahara desert. Seasonal wind patterns make these episodic events more frequent in winter and summer (Neuer et al., 2004).

The NASTE presents weak annual variability in physical, chemical, and biological conditions (Longhurst, 2007; Marañón et al., 2007). Apart from the exceptional events mentioned above, enhanced turbulent mixing promotes a slight phytoplankton bloom in winter. Also, and especially at the southeastern boundary of the NASTE, advection is important for nutrient renewal within the gyre (Pelegrí et al., 2006). Another potential mechanism is salt-fingering, although its importance remains less explored (Oschlies et al., 2003). On the other hand, CNRY is one of the most productive regions in the world because of permanent upwelling. In this way, the seasonal migration of trade winds promotes an enhancement of upwelling, with two peaks of productivity, in spring and autumn (Longhurst 2007). These peaks are also associated with enhanced nutrient supply to the gyre (Pelegrí et al., 2006).

2.2. Water-column physical, chemical, and biological conditions

At each station, temperature, salinity, fluorescence, and oxygen profiles to 300 m were obtained from a SBE-19 CTD, equipped with a SeaPoint fluorometer and an SBE-43 oxygen meter. The CTD was mounted on a rosette with 24 Niskin bottles of 12 L from which seawater samples were obtained at several discrete depths (5, 50, and 200 m, and three depths selected to characterize the deep chlorophyll maximum; see Table 1). Water for nutrient analysis was collected in polystyrene tubes, which were immediately frozen and preserved at $-80\,^{\circ}$C. Nitrate, nitrite, and phosphate concentrations were determined using a Technicon AAII autoanalyser following the methods described by Tréguer and Le Corre (1975); with detection levels of 2 nM for nitrite, 5 nM for nitrate, and 20 nM for phosphate. Oxygen concentration was measured using Winkler's method (see Grasshoff, 1983) to calibrate the SBE-43 oxygen sensor (R^2=0.96) and to derive oxygen saturation. Finally, size-fractionated Chl *a* concentrations (0.2–2.0 and $>2.0\,\mu$m) were estimated by filtering 250 ml of seawater through Millipore polycarbonate filters. Each filter was immediately submerged in pure acetone and left in the dark at $-80\,^{\circ}$C for $8-12$ h. Chlorophyll *a* concentration was then determined by the fluorescence method (Yentsch and Menzel, 1963) using a Turner Designs (TD-2400) fluorometer.

2.3. Characterization of Trichodesmium population structure

Plankton samples were obtained at midday (10:30 GMT) using a 53 μm mesh, 0.30 m diameter mouth triple WP_2 net (Fraser, 1966) towed vertically from 200 m. Because one of our primary objectives was the inclusion of reliable measurements of the abundance of *Trichodesmium* colonies and free trichomes, nets were towed at a relatively slow speed ($0.5\,m\,s^{-1}$). Despite this, colony damage and fragmentation or the escape of free trichomes through the mesh cannot be completely ruled out (Tangen, 1978). Also, given the speed of net tows, there could be an overestimation of the volume of water filtered due to clogging. Nets were nevertheless preferred over bottle samples (see below), which are known to result in biased estimates of colony abundance (Chang, 2000). At the surface, nets were gently washed, and the cod-end content was retrieved and preserved with 4% buffered formaldehyde seawater until further processing.

Each entire sample was examined under a stereo microscope (Leica Z12.5) to enumerate *Trichodesmium* colonies (puffs and tufts). A 10% aliquot of the whole sample was taken to record the number of free trichomes. To enumerate the amount of trichomes forming tuft or puff colonies, up to ten colonies of each type were isolated, gently disaggregated, and counted. These colony-forming trichomes, as well as a representative number of free trichomes (n=40), were photographed under the microscope. The length and width of each trichome was then measured to the nearest micrometer using digital imaging software (Image-Pro Plus, Media Cybernetics). Unfortunately, during these operations, two samples (E3 and E6) were mixed and had to be discarded.

2.4. Large-scale surface conditions

In situ environmental data were complemented with remote sensing images. We retrieved data on wind stress fields, sea surface temperature (SST), aerosol optical thickness (AOT), chlorophyll *a* concentration, *Trichodesmium* bloom occurrence, and dynamic surface topography. These data summarized large-scale variation during our field sampling and also regional conditions before and after we occupied each station. In all the cases, we took a subset the original data from the window defined by the points 45°N 50°W and 15°N 0°. Depending on availability, daily or weekly data was used and averaged for the period of sampling. Weekly data was preferred to explore the conditions both up to 6 months before and 2 months after *in situ* sampling.

Daily, 0.25° gridded wind speed and direction fields were obtained from QuickSCAT scatterometer (i.e. a specialized radar sensor; see Liu and Xie, 2006) L3 data, processed at the Jet Propulsion Laboratory (JPL, California Institute of Technology, NASA; winds.jpl.nasa.gov). Wind stress fields serve as a proxy of wind-

driven divergence and Ekman pumping, which could cause local increases in nutrient concentration and relax phytoplankton competition.

Daily and 8-day-averaged MODIS sensor fields mapped into a 4 km grid were obtained from the Ocean Color Web (Feldman and McClain, 2008; Goddard Space Flight Center, NASA; oceancolor.gsfc.nasa.gov). Retrieved MODIS variables included SST, AOT at 869 nm, Chl *a*, normalized water-leaving radiances in the visible range (nLw at 412, 443, 448, 531, 551, and 667 nm), the Angstrom coefficient at 531 nm ($Å_{531}$), and the aerosol correction factor (ε). Daily data was used to build an average map during sampling, while weekly averages were employed to explore past conditions and to apply bloom detection algorithms. Sea surface temperature, apart from serving as a tracer of ocean dynamics, is an important variable influencing physiological processes and constrains *Trichodesmium* ability to fix N_2 (Breitbarth et al., 2007). Aerosol optical thickness measures the amount of light absorbed by particles suspended in the atmosphere and thus serves as a proxy for dust deposition. The MODIS AOT product employed here is a standardized parameter (range 0–1), with AOT ≤ 0.1 indicating nearly clear sky conditions and values near 1.0 indicating heavy haze. It should be noted that phytoplankton also produces aerosols (Simó, 2001), so in some cases the cause and consequence of variations in AOT can be difficult to discern (Volpe et al., 2009). Because of the high requirements of iron by the nitrogenase system, the deposition of dust particles rich in iron is expected to promote *Trichodesmium* growth. Chlorophyll *a* concentration serves as a measure of phytoplankton biomass. Like SST, it serves as a tracer of large-scale and mesoscale oceanographic features. Finally, we employed the semi-analytical algorithm developed by Westberry et al. (2005) (hereafter WSS05) to identify potential areas that can be interpreted as *Trichodesmium* blooms. The empirical threshold employed by Wilson and Qiu (2008) (monthly or weekly Chl *a* concentration greater than 0.15 mg m^{-3}) was also used to search for generic blooms in the region sampled.

Altimeter products, mapped in a 0.33° Mercator grid, were produced by Ssalto/Duacs and distributed by *Aviso* (www.aviso.oceanobs.com), with support from *Cnes*. We employed weekly averaged fields obtained by merging data from various missions (Topex/Poseidon, Jason-1, European Remote Sensing satellites [ERS 1 and 2], and Envisat) using the methods developed by Le Traon et al. (1998). Dynamic topography provides a portrait of surface circulation and of the presence and importance of mesoscale features. These data can thus help in identifying processes that can alter the local nutrient regime or advect waters and organisms from other locations. We used merged sea surface heights (MSSH) and anomalies and the derived geostrophic velocities to study the possible influence of mesoscale structures during sampling. These variables were used to estimate eddy kinetic energy (EKE) and the Okubo-Weiss parameter (W) (Isern-Fontanet et al., 2003). This last quantity is a measure of the relative importance of deformation and rotation in the flow. It is estimated as the difference between the sum of the squared normal and shear components of strain, and the square of relative vorticity. Eddies are identified as closed contours of negative W values (i.e. regions dominated by vorticity), which can then be followed in time (see Isern-Fontanet et al., 2003).

2.5. Data analysis

All the data were arranged jointly before analysis, and each variable was summarized in a unique value for each station. For water-column physical, chemical and biological variables, values were averaged using Riemann integration within the mixed layer, which depth was determined by finding the maximum Brunt-Väissälä frequency (Pickard and Emery, 1990). For satellite data, values corresponding to the location of each station were interpolated using splines, while large-scale and detail maps were produced to examine surface conditions in a wider extent.

In all the analyses, we focused on *Trichodesmium* abundance and size, which were set as the dependent variables when appropriate. We also studied variation in population and size structure by estimating the percentage contribution of each component (i.e. free trichomes, puffs and tufts). In this case, we obtained total population densities by previously transforming the data to standardized units of abundance (number of trichomes) and size (total volume) for each component per square meter. The possible differences in *Trichodesmium* mean sizes at each station were tested using a generalized linear model with log link (i.e. normality assumption). Station was included as a fixed effects factor, i.e. we assumed it represents a limited array taken from all possible ones. The identity of each tuft and puff was also included as a random effects factor when size variation in these forms was analyzed. This last factor allowed an *ad hoc* control of possible correlation within each colony because of autocorrelation in measurement errors and also allowed accounting for systematic differences in trichome size between colonies. The inclusion of environmental covariates in these models was avoided because of the small sample size. The significance of fixed effects factors was assessed using an F test. Likelihood ratio tests (LRT) were used to assess the reliability of random effects (Venables and Ripley, 2002).

Trichodesmium N_2 fixation rates were estimated indirectly using published values because of the lack of concurrent measurements. Our objective was to obtain approximate estimates of fixation rates from the abundances recorded and, employing a heuristic approach, from variations in size (Orcutt et al., 2001; Goebel et al., 2007) and environmental temperature (Breitbarth et al., 2007). Thus, the values obtained should be interpreted cautiously and not as absolute quantities. To estimate variation in N_2 fixation rates from the abundances and sizes recorded, we employed an intermediate equivalence of 0.30 nmol N colony^{-1} h^{-1}. This is a compromise with the rates of 0.25–0.35 nmol N colony^{-1} h^{-1} recommended by Kolber (2006), derived from the ranges of 0.03–0.74 and 0.04–0.80 nmol N colony^{-1} h^{-1} reported by Orcutt et al. (2001) for puffs and tufts, respectively. Also following Orcutt et al. (2001), we applied an equivalence factor of 0.33 between free and colony-forming trichomes to estimate N_2 fixation rates for this component of *Trichodesmium* populations. This value was selected as a compromise between those reported by Saino and Hattori (1982), 0.37, and Letelier and Karl (1998), 0.28. Finally, to estimate the potential impact of size variation in N_2 fixation rates, we applied the thermodynamic and allometric principles advocated by the metabolic theory of ecology (e.g. Brown et al., 2004). We obtained raw estimates of the proportional contribution of each morphotype to total N_2 fixation based on the corrections derived from this theory for changes in trichome size and environmental temperature by adjusting the total nitrogen fixation predicted by considering only abundance variation (see Appendix A for further details).

All calculations and data processing were done in Matlab R2008 (MathWorks Inc., 2008), except for linear models, which were fitted in *R* (*R* Development Core Team, 2008), using the package *nlme* (Venables and Ripley, 2002).

3. Results

3.1. Oceanographic conditions

The physical conditions during the CARPOS cruise encompassed a gradient between near temperate, beginning at the north of the Azores front, to fully subtropical conditions towards the

interior of the northern subtropical gyre (Figs. 1 and 2). This was reflected in a trend towards increased temperatures and salinities in a shallower mixed layer, which were accompanied by subtle changes in physical, chemical, and biological variables (Table 1). A heuristic boundary for the gyre is depicted in Fig. 2b (pink contour), based on the criteria used by McClain et al. (2004) (i.e. Chl $a > 0.08\ \mathrm{mg\,m^{-3}}$), which indicated that the first stations were close to the gyre boundary, whereas the remainder were within the gyre except for station E5.

Satellite images of sea surface temperature and Chl *a* (Fig. 2) reflected weak changes in surface conditions, as well as reduced wind stress south of 30°N, and a near absence of aeolian dust deposition at our sampling sites during the cruise (Table 1). Although values of aerosol optical thickness were higher towards the interior of the gyre, their magnitude was always around 0.1, indicating that dust deposition was negligible. Examination of fields corresponding to the 2 weeks before we occupied each station also indicated that both wind-driven divergence and atmospheric nutrient deposition were not important. The contribution of small phytoplankton (Chl $a < 2\,\mu\mathrm{m}$) remained nearly constant (range 65–68% for stations E0 to E6), as Chl *a* concentration decreased as we entered the subtropical gyre, with the exception of E7, in which the percentage decreased to 59%. Inorganic nutrient concentrations were very low in the mixed layer throughout the transect (Table 1), especially PO_4, which mean concentration was bellow the detection limit (20 nM) from E3 onwards (see also Figure S1 in the Online Appendix).

All the observed changes were gradual except for station E5, which presented a sharp discontinuity in all the physical, chemical, and biological parameters studied (Fig. 3), including *Trichodesmium* abundance and size (see below). Indeed, this station was identified as a *Trichodesmium* bloom by the analytic algorithm of Westberry et al. (2005) (WSS05) (Fig. 4), although not by the criteria employed by Wilson and Qiu (2008) (purple line contour in Fig. 2b). The highest salinity and potential temperature values in all the transect were found at this station. This is even more striking if we consider its location, and the extent of the anomaly throughout the photic zone, with salinity values greater than 37 in the first 150 m of the water-column. A discontinuity in the subsurface oxygen saturation was also apparent, as well as an increase in Chl *a* concentration with respect to adjacent stations (Table 1).

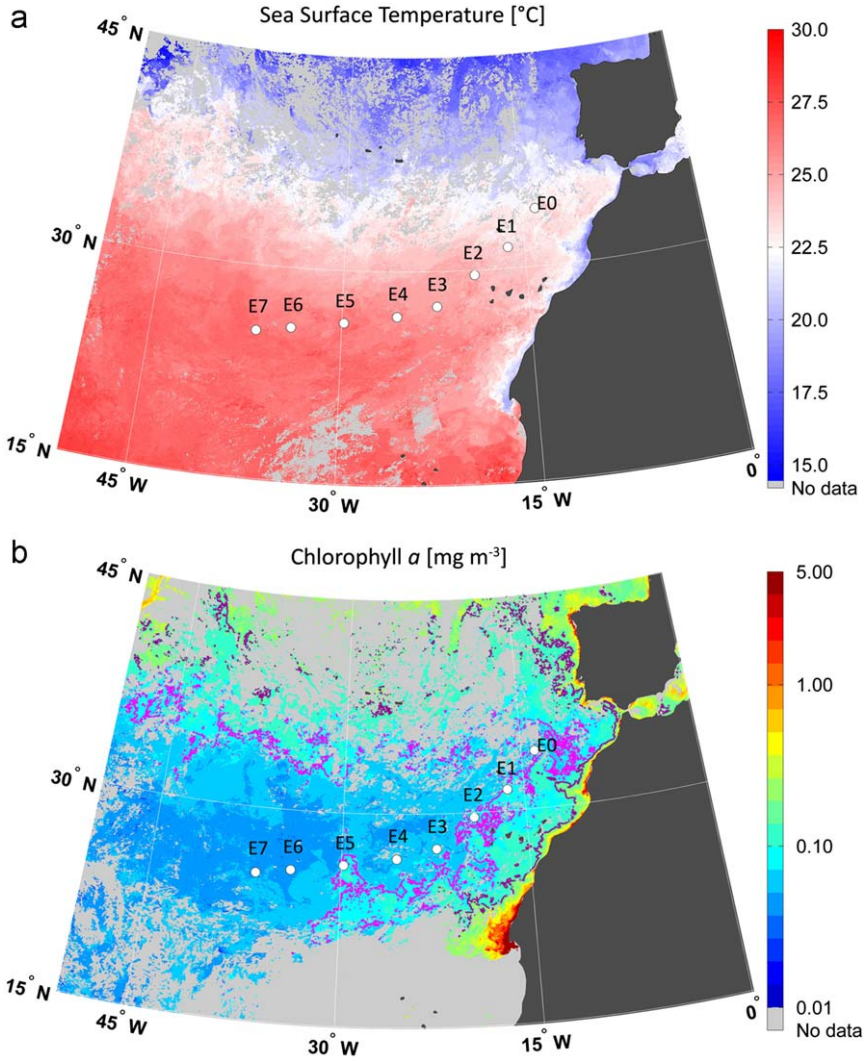

Fig. 2. Remote sensing satellite images used to define large-scale surface conditions: (a) sea surface temperature [°C]; (b) chlorophyll *a* concentration [$\mathrm{mg\,m^{-3}}$]. Pink and purple contours correspond to 0.08 and 0.15 $\mathrm{mg\,m^{-3}}$ Chl *a*. These concentrations have been used to map the extent of the subtropical gyre (McClain et al., 2004) and the occurrence of blooms in subtropical zones (Wilson and Qiu, 2008), respectively. Daily images between 14 October 2006 and 21 October 2006 were averaged. MODIS data were obtained from the Ocean Color Web (Feldman and McClain, 2008). (For interpretation of the references to colour in this figure legend, the reader is referred to the web version of this article.)

Table 1
Variations in physical, chemical, and biological conditions along the transect.

	West			Station			*East*	
	E7	E6	E5	E4	E3	E2	E1	E0
Location	36.7°W, 25.4°N	34.0°W, 25.8°N	29.8°W, 26.3°N	25.6°W, 26.8°N	22.4°W, 27.5°N	19.3°W, 29.7°N	16.4°W, 31.5°N	13.9°W, 34.1°N
Day of October 2006	21	20	19	18	17	16	15	14
MLD (m)	56.6	55.6	57.6	66.6	48.6	57.5	60.5	50.6
Pot. T (°C)	26.08	25.80	25.91	24.78	24.98	23.95	23.88	23.30
Salinity	37.392	37.523	37.481	37.400	37.318	37.067	36.911	36.854
σ_t (kg m^{-3})	24.81	25.00	24.93	25.22	25.10	25.22	25.12	25.25
O_2 (%)	102.54	102.68	102.73	103.48	102.05	103.58	102.09	103.06
Chl *a* (mg m^{-3})	0.070	0.111	0.235	0.127	0.134	0.186	0.237	0.240
Depth of the DCM (m)	140	135	100	110	108	100	100	95
NO_2+NO_3 (nM)	249	250	241	251	–	245	238	–
PO_4 (nM)	–	≤ 20	≤ 20	≤ 20	≤ 20	30	40	–
AOT (unitless)	0.06	0.07	0.11	0.03	0.03	0.05	–	–
Wind (m s^{-1})	3.28	3.13	4.14	3.54	3.51	4.36	5.94	6.84
MSLA (cm)	6.6	6.6	10.5	7	9.1	12.7	6.9	4.7
AGV (cm s^{-1})	2.0	4.0	4.7	5.7	4.5	3.3	8.1	18.6
EKE (cm^2 s^{-2})	10	14.3	17	7.1	22.1	24.5	18.1	189.2

All values derived from direct sampling in the field were averaged for the portion of the water column encompassing the mixed layer, while satellite derived variables, which only report surface conditions for a given area, were obtained for each spatial/temporal location using spline interpolation on data averaged for the sampling period (see Materials and methods for details). *Abbreviations*: MLD, mixed layer depth; Pot. T., potential temperature from ITS90 standard; Chl *a*, total chlorophyll *a* concentration; DCM, deep chlorophyll maximum; AOT, aerosol optical thickness; SLA, sea level anomaly; AGV, absolute geostrophic velocity; EKE, eddy kinetic energy.

This set of characteristics suggests the presence of a different water body at station E5. In this area there was also a positive sea level anomaly and a convergent circulation pattern (Fig. 5a). The Okubo-Weiss (W) parameter confirmed the dominance of rotation over deformation in the flow. We searched the origin of this anticyclonic eddy following the closed contour of negative values of W back in time. The analysis revealed that the eddy was propagating westward with velocities around 100 km per month, and that it was associated with a cyclonic eddy originated in the Canary archipelago. Thus, this anomaly was probably a shallow subtropical subducting westward propagating eddy (*swesty*), as described by Pingree (1996; see also Pingree and García-Soto, 2004). Because the origin of the sea level anomaly does not explain the values found for either temperature or salinity at E5, we further explored geostrophic velocity fields back in time. We found that, nearly a month before we occupied station E5, the anticyclonic gyre was under the influence of a northward current flowing from the southern boundary of the subtropical gyre (Fig. 5b and c). This was confirmed by following back in time the *Trichodesmium* bloom found at station E5 as detected by the WSS05 algorithm (Fig. 4). Following the bloom forward (not shown) revealed that *Trichodesmium* remained trapped in the *swesty* before vanishing after a few weeks.

3.2. Trichodesmium *abundance, size, and derived N_2 fixation rates*

Along all the transect, temperature was above 20 °C, which sets the threshold from which N_2 fixation becomes an efficient process for *Trichodesmium*. Up to station E1, any *Trichodesmium* colonial form was found. The abundance of all components of *Trichodesmium* populations increased from its appearance steadily, except for a sharp increase at station 5 (Fig. 6a). In all samples, free trichomes were the dominant component, although the numerical importance of colonies increased towards the interior of the gyre. Puffs appeared at E2 while tufts at E4, and although at this station puffs were numerically more abundant, tufts represented a greater component in terms of volume. Towards the interior of the gyre, tufts became more abundant than puffs and, at the last station, they were nearly as important as free trichomes in both number and volume (Fig. 6a and b).

The changes in ocean conditions at station E5 were also reflected in *Trichodesmium* abundance, and indeed, abundances of all morphotypes peaked at this site. The different size measurements showed marked trends in each component of *Trichodesmium* populations (Fig. 6c and d). The volume of both free trichomes and tuft-forming colonies increased towards the centre of the gyre ($F_{3,156}$=13.7 and $F_{2,22}$=17.4, respectively; $p<0.05$) after controlling for significant individual effects in tufts (LRT, χ^2=16.4, df=1, $p<0.05$). Mean free trichome volume increased by a factor of $\sim$1.7 from station E2 to E7 (1682 ± 448 and 2907 ± 611 μm^3 [mean $\pm$ SE], respectively). For tufts, mean trichome volume was similar between stations E4 and E7, although the mean number of trichomes per tuft nearly doubled (from 31 ± 9 to 63 ± 10). For both free trichomes and tuft-forming trichomes, mean volume increased at station E5. Although the abundance response was similar to that found for the other morphotypes, trichomes forming puffs presented no significant variation in mean volume (range 360–450 μm^3; $F_{3,25}$=1.24, p=0.32, but significant individual effects LRT, χ^2=176.5, df=1, $p<0.05$) and a unimodal pattern in the number of trichomes per puff, which peaked at intermediate stations.

Abundance-based N_2 fixation rates ranged from 0 nmol N m^{-2} h^{-1} at station E0, to 4408 nmol N m^{-2} h^{-1} at station E5, although the value found at station E7 was of only 964 nmol N m^{-2} h^{-1} (Table 2). At station E5, tufts showed the maximum contribution of any morphotype, with a value of 1829 nmol N m^{-2} h^{-1}.The percentage contribution of the different components also varied, with both free trichomes and puffs decreasing their relative importance towards the interior of the gyre, where tufts accounted for 56% of N_2 fixation. When the abundance-based total N fixed was partitioned among morphotypes and stations based on changes in size and temperature, the results varied widely for different stations (Table 2).

The residual mean square (RMS) between abundance-based estimates and those corrected by size and temperature variation was $RMS_{T,\ Size}$=260.1. The deviation of these estimates from abundance-based ones was much more sensitive to the assumption of trichome size as constant along the transect than to that of constant temperature ($RSM_{T,\ Size\ fixed}$=259 and $RMS_{T\ fixed,\ Size}$=293, respectively). Thus, the variations between different estimates were mainly due to the inclusion of size dependence in the

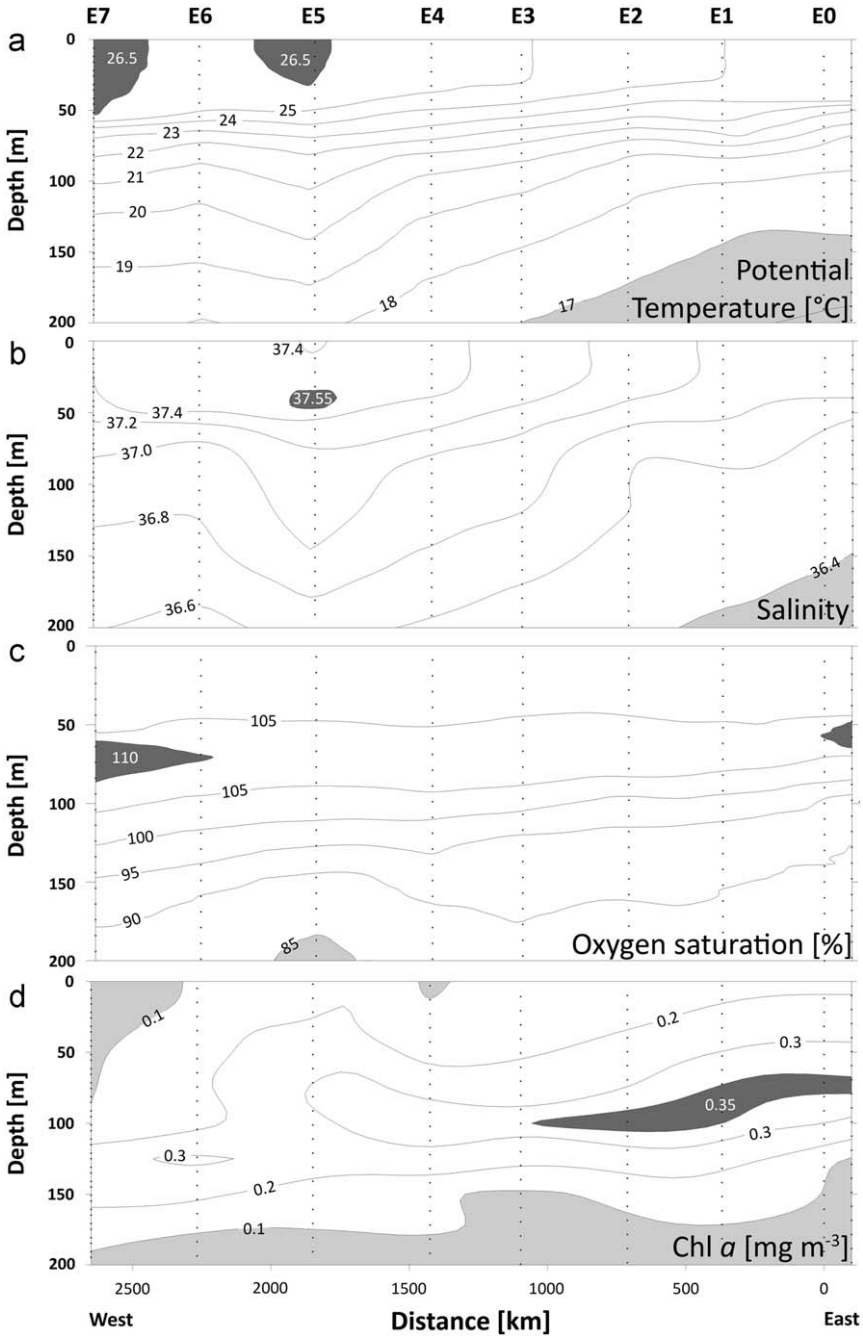

Fig. 3. Water-column physical, chemical and biological conditions derived from *in situ* data: (a) potential temperature (ITS90 standard) [°C]; (b) salinity; (c) oxygen saturation [%]; and (d) total chlorophyll *a* concentration. Contour plots were interpolated using kriging.

derivation of N_2 fixation rates. In general, estimated fixation rates increased at all the stations except E5, which showed a 9% decrease. The most extreme case occurred at station E4, which doubled the abundance-based estimate, due to the greater weight assigned to free trichomes. Also, the maximum fixation rate was assigned again to station E5, but in this case free trichomes were the most important N_2 fixers (2151 nmol N m^{-2} h^{-1}).

4. Discussion

Trichodesmium patterns of abundance, size structure, and the indirect N_2 fixation rates, varied systematically throughout the gradient in environmental conditions established between the Azores front and the interior of the northern subtropical gyre. Rather than a gradual transition, mesoscale features and advection altered these patterns locally, especially at one of our stations. We devote the rest of the paper to discussion of our observations on *Trichodesmium* population structure, to compare our results with previous work, emphasizing especially the contrast with the western side of the gyre, and to statement of the implications of our results for future studies in the eastern subtropical North Atlantic.

4.1. Trichodesmium *abundance in the eastern subtropical North Atlantic*

Tyrrell et al. (2003) reported abundance measurements that matched relatively well with those found here. A direct

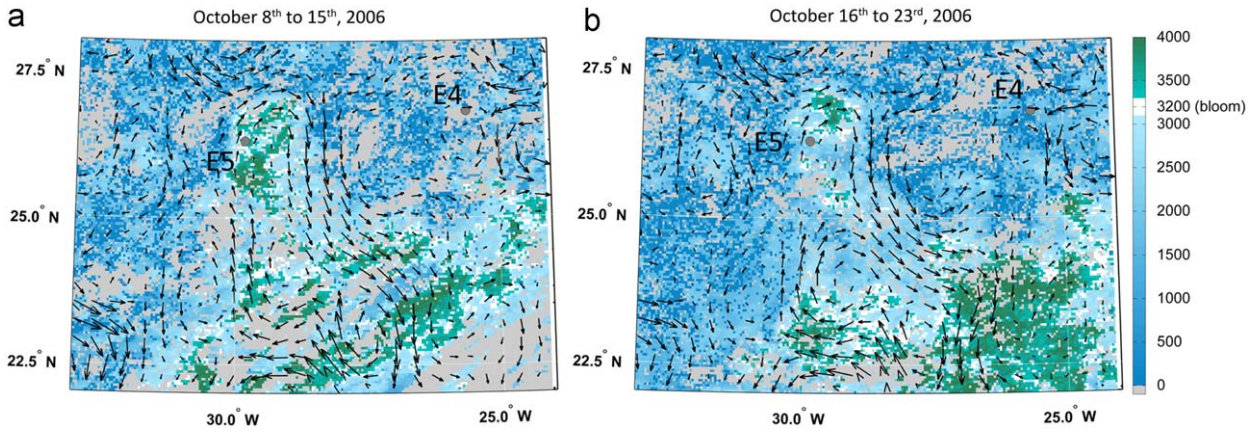

Fig. 4. *Trichodesmium* abundance as retrieved by the semi-analytic algorithm of Westberry et al. (2005). A pixel is considered to correspond to a *Trichodesmium* bloom when trichome concentration is above 3200 trichomes L^{-1} (green tones), which are contoured in the maps by a white line. Panel (a) corresponds to the situation a week before (October 8–15, 2006), we occupied station E5 while panel (b) is nearly synoptic with the *in situ* measurements taken on October 19 (October 16–23, 2006). Arrows correspond to the orientation and magnitude of geostrophic velocities. Data from the Ocean Color Web (Feldman and McClain, 2008; MODIS data employed to identify *Trichodesmium* blooms) and AVISO/DUACS (dynamic topography).

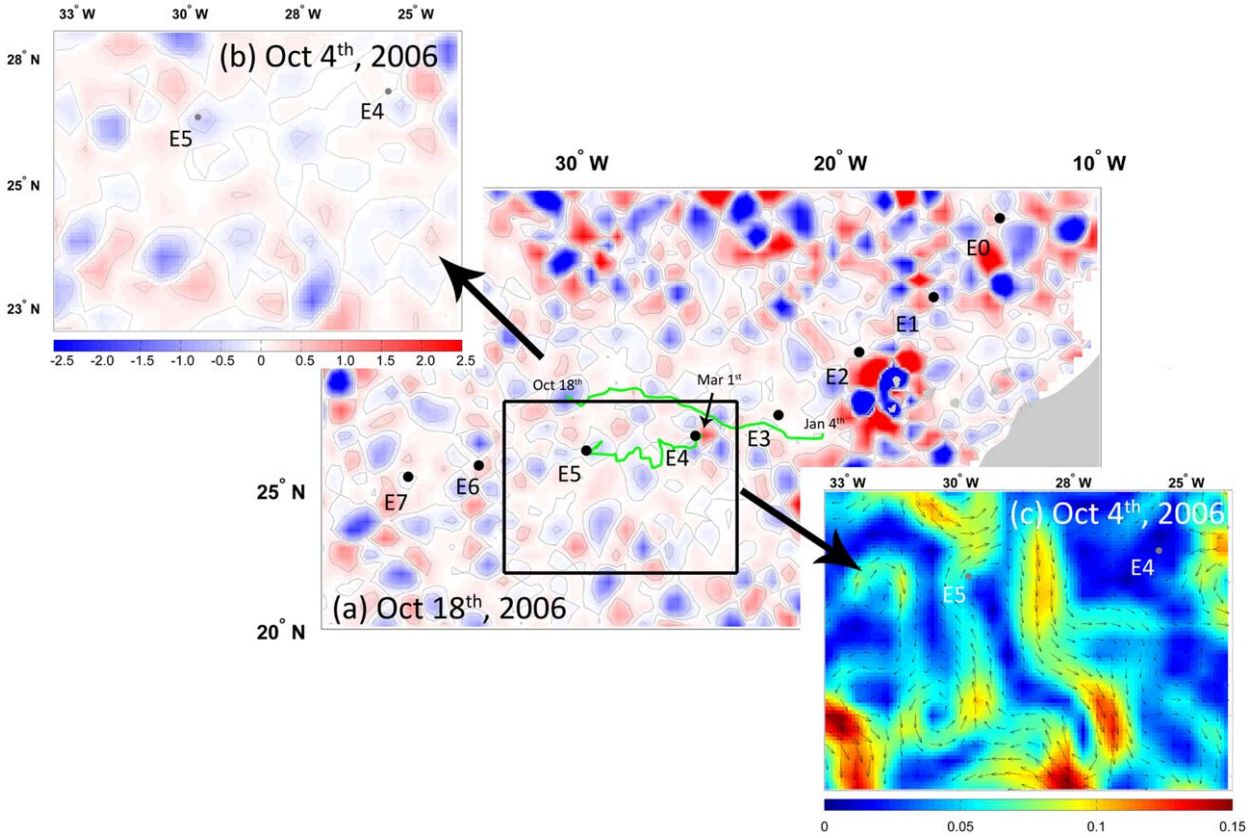

Fig. 5. Surface circulation and mesoscale structures during the transect as inferred from dynamic topography satellite images. The main panel (a) presents values of the Okubo-Weiss parameter nearly the day we occupied station E5 (October 19, 2006) [multiplied by 10^{11}; note that the scale is shown in panel (b)]. Contours of $\pm W_0$ separate regions of the flow dominated by deformation (red) or rotation (blue). The value of W_0 is based on the observed standard deviation of the Okubo-Weiss parameter in the region (W_0=0.2σ_W; see Isern-Fontanet et al., 2003). The green lines represent derived trajectories using an automatic algorithm for the two mesoscale structures discussed in the text. Panels (b) and (c) correspond to the region enclosed in (a) by a rectangle. They present the Okubo-Weiss parameter (a) and surface circulation patterns (c) 3 weeks before the anomaly reached station E5 (October 4, 2006). In (c), arrows and color grades correspond to the orientation and magnitude of geostrophic velocities. Data courtesy of AVISO/DUACS. (For interpretation of the references to color in this figure legend, the reader is referred to the web version of this article.)

comparison is difficult, since most of their data consists in bottle samples closed near the surface and at the deep chlorophyll maximum (Tyrrell et al., 2003), while the nets we employed are prone to underestimation of the concentration of free trichomes. Nevertheless, free trichome abundances were in general of the same order of magnitude as those reported here. Indeed, the values found towards the interior of the gyre matched well with the mixed layer average estimated by Tyrrell et al. (2003) for the region between 0° and 15°N (range, $1.7\times10^5-8.5\times10^6$ against 1.8×10^5–1.4×10^6 free trichomes m^{-2} found here between stations E5 and E7, located at ~25°N). For northern latitudes, the Tyrrell et al. (2003) abundance estimates were in general lower. In

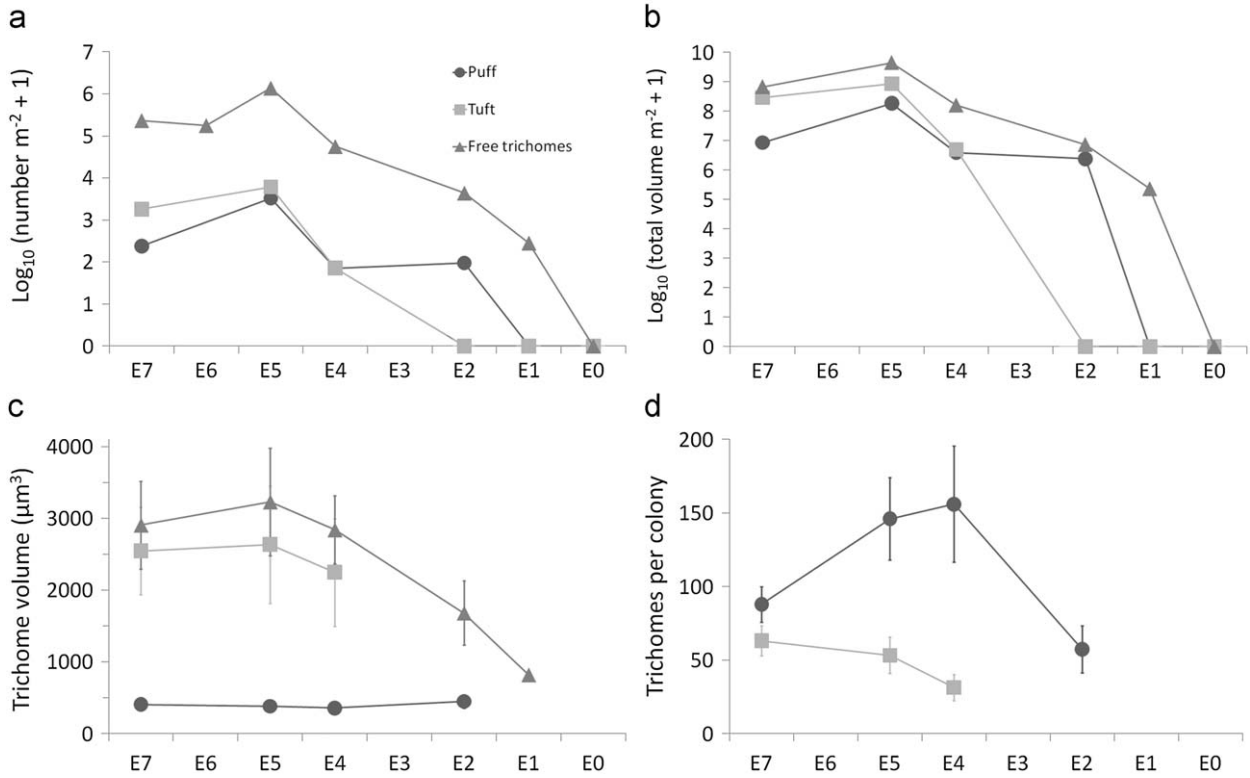

Fig. 6. *Trichodesmium* abundance and size structure along the transect. (a) Abundance-based density estimates for free trichomes, tufts and puffs (note that data were Log_{10} transformed and that is presented as number m^{-2}). (b) The same as (a), but converting abundance-based density units to total trichome volume [note the Log_{10} scale; units, $\mu m^3\,m^{-2}$]. (c) Mean trichome volume [μm^3] for each of the components of the population. (d) Number of trichomes per colony. Where present, bars correspond to standard-error-based confidence intervals.

Table 2
Estimates of *Trichodesmium* spp. N_2 fixation rates (nmol N $m^{-2}\,h^{-1}$) derived by two different methodologies.

Station	Indirectly derived N fixation rates [nmol N $m^{-2}\,h^{-1}$]							
	Abundance-based estimates				*Size- and temperature-adjusted estimates*			
	Puff	Tuft	Free trichomes	*Total*	Puff	Tuft	Free trichomes	*Total*
E0	0.0	0.0	0.0	0.0	0.0	0.0	0.0	0.0
E1	0.0	0.0	0.5	0.5	0.0	0.0	1.2	1.2
E2	28.3	0.0	7.6	35.9	15.6	0.0	15.6	31.3
E3	–	–	–	–	–	–	–	–
E4	21.2	21.2	59.2	101.6	23.8	28.2	164.7	216.7
E5	988.9	1829.2	1590.2	4408.3	454.2	1434.6	2151.3	4040.1
E6	–	–	–	–	–	–	–	–
E7	72.2	543.2	348.7	964.1	46.1	646.1	529.1	1221.2

Rates were indirectly derived from abundance data (left), and also including size and temperature corrections (right). Because with the second approach we could only establish the scaling of N_2 fixation rates with size and temperature up to a multiplicative constant, these values were adjusted to the total sum retrieved by the classic method. Note that we estimated colony size by free trichome volume. See Materials and methods and Appendix A for further details.

this way, although we cannot reject any impact due to the loss of free trichomes through the mesh, our values were in the range of those previously reported for the nearest regions. Our results were also similar to those by Davis and McGillicuddy (2006) except for a few aspects, and considering only the data up to 40°W. Puffs were the dominant component of *Trichodesmium* populations, contrary to what was found here at the westernmost stations. Also, the maximum concentration found at station E5 (i.e. 16 puffs and 30 tufts m^{-3}) was higher than most of the values reported by Davis and McGillicuddy (2006) for the eastern North Atlantic. It should be noted that they found a clear relationship between colony abundance and positive sea level anomalies.

Both the reduced sample size and the subtle variation in most of the physical and chemical variables examined prevented a more elaborate analysis of the effect of environmental conditions. In their latitudinal analysis of data from several years, Tyrrell et al. (2003) concluded that dust deposition and mixed layer depth are the main factors responsible for changes in *Trichodesmium* abundance. It should also be stressed that the Tyrrell et al. (2003) samples at these latitudes were located near the African coast (~20°W). The nearly longitudinal transect conducted here does not support the same conclusion. Indeed, *Trichodesmium* abundance increased towards the interior of the gyre, where external iron inputs are less important than near the coast (Mahowald et al., 2009). During the cruise, aeolian deposition was not apparent, and variation in mixed layer depth was very weak (Table 1). Thus, different factors can generate both gradients although, with the data at hand, we can only conclude that conditions towards the interior of the gyre seem to favour *Trichodesmium*.

The observed trend in *Trichodesmium* abundance was more than a simple increase towards the interior of the gyre. Different morphotypes appeared in a specific order as we progressed towards the interior of the gyre; free trichomes appeared first, while puffs and tufts were found far west. When present, tufts were dominant in terms of volume, although puffs were numerically more abundant near the eastern boundary of the gyre. This reconciles our observations with the dominance of puffs found by Davis and McGillicuddy (2006) near the Azores front. Jointly, these results suggest that puffs present a certain kind of competitive advantage over tufts near the boundaries of the gyre, and that they are displaced by tufts towards the interior of the

gyre. This idea was reinforced by consideration of the number of trichomes per colony towards the interior of the gyre, which showed a linear increase in tufts, but a humped relation for puffs.

Finally, we found bloom conditions associated with positive sea level anomalies, which we identified with a *swestie*, as described by Pingree (1996). This resembled the results in Davis and McGillicuddy (2006), although it should be stressed that their transect ran parallel to the Azores front and crossed the Gulf Stream, regions with greater eddy kinetic energy. As deduced from examining remotely sensed dynamic topography, the origin of this anomaly was not compatible with the potential temperature and salinity signatures observed. Although the maintenance of *Trichodesmium* blooms is probably related to eddy/wind interactions (McGillicuddy et al., 2007), this particular bloom seems to be related to the advection and local retention of *Trichodesmium* from denser, southern populations (Tyrrell et al., 2003), rather than to local enhancement of nutrient concentrations. The application of the WSS05 algorithm to detect *Trichodesmium* blooms reinforced this notion.

4.2. *Comparison with* Trichodesmium *studies in the western subtropical North Atlantic*

Abundances reported for the western side of the North Atlantic subtropical gyre were of the same order of magnitude as those found here for the eastern side. In general, our values were slightly higher than those found in bottle samples by Carpenter et al. (2004) (i.e. mean of 730 colonies m^{-2} derived for October, tropical [north of 23°N and west of 40°W]; versus the 241 puffs and 1811 tufts m^{-2} found in this study in the interior of the gyre). There was a clear exception at station E5, where we estimated a colony concentration of 3296 puffs and 6097 tufts m^{-2}. These figures were also well above the abundances reported during the seasonal bloom (maxima of 1111 m^{-2}) by Orcutt et al. (2001), who used nets to sample *Trichodesmium* abundance.

Trichodesmium colony abundances reported here were lower than the values found by Davis and McGillicuddy (2006) for the northern margin of the western subtropical North Atlantic (abundances as high as 35 puffs and 85 tufts m^{-3} at the Gulf Stream front, versus our maximum at station E5 of 16 puffs and 30 tufts m^{-3}). Nevertheless, it should be noted that the sampling methods employed in all these studies differed greatly from those used here; i.e. 1 m mouth, 335 μm mesh in Orcutt et al. (2001); 10 L of bottle-sampled seawater in Carpenter et al. (2004); and the Visual Plankton Recorder [VPR] in Davis and McGillicuddy (2006).

4.3. Trichodesmium *size structure and indirect N_2 fixation rates*

Our characterization of size structure matched values reported in previous studies, although we have not found previous estimates of the variation in trichome volume. Letelier and Karl (1996) found a mean value of 182 trichomes per colony (range 10–375) at station ALOHA, which is slightly higher than that found here (112 ± 47 for puffs [range 57–156], and 49 ± 16 for tufts [range, 31–63]). Our values are nevertheless in better agreement with the values reported by Carpenter et al. (2004) (98 ± 11; range, 53–153) for the North Atlantic. The volume of free and tuft-forming trichomes, and of the number of trichomes per puff or tuft, increased towards the interior of the gyre. Mean trichome volume also increased for tufts and free trichomes towards the interior of the gyre, although it remained nearly constant in puffs. Indeed, size variation in puffs was driven by changes in the number of trichomes per puff, which peaked at station E4. This occurred before fully subtropical conditions were attained and before either free or tuft-forming trichomes reached their maximum size. These patterns reinforce the idea of an alternation of the different morphotypes from temperate to subtropical conditions, with puffs being favoured by the conditions at the border of the gyre.

Water-column integrated N_2 fixation rates indirectly derived from abundance estimates were also higher than those reported for the western side of the gyre by Orcutt et al. (2001), although the rates we estimated were very similar to those reported during bloom conditions (i.e. >2000 nmol N m^{-2} h^{-1}; derived from monthly values at BATS). Although we found a slightly lower contribution of free trichomes to N_2 fixation rates with respect to the 75% reported by Orcutt et al. (2001), the percentage contribution was nevertheless important, ranging from 21% to 58% in abundance-based estimates, and from 43% to 76% in size- and temperature-corrected ones (note that we have ignored station E2, where colonies were absent). Finally, despite the exploratory character of indirect estimates of N_2 fixation rates including the effect of size and temperature, two important ideas emerged from it. First, allowing an effect of size on N_2 fixation rates can produce variations in estimates of 100% when compared to estimates based only on abundance. Second, free trichomes represent a more important component of *Trichodesmium* populations when size is considered.

4.4. *Implications*

Our study had a limited extent and duration, so any conclusion extracted from it should be carefully considered. Nevertheless, it yields two important messages. First, it underlines the importance of combining *in situ* measurements with other data sources. Here we used remote sensing data to interpret our *in situ* measurements in a wider oceanographic context. This was the case of the *Trichodesmium* bloom, which at a first sight seemed to be related to some type of eddy pumping. By combining *in situ* data with remotely sensed dynamic topography and *Trichodesmium* bloom occurrence, we were able to reconstruct previous conditions and relate the origin of the bloom to the northward advection of *Trichodesmium*-rich waters.

On the other hand, after a review of the recent literature, sampling issues appeared as one key determinant of *Trichodesmium* studies. Indeed, these species present positive buoyancy, great size and low concentrations in the water-column with respect to other phytoplankton groups; they are delicate and can be fragmented easily, they adhere to containers, etc. In this sense, bottle sampling has been criticized because the low volume of water sampled can introduce a bias in colony abundance estimates (Chang, 2000). On the other hand, nets could promote colony fragmentation and allow the escape of free trichomes through the mesh and on occasion the volume filtered can be overestimated because of clogging. All these problems, which also affected our own study, can alter as well abundance estimations based on net sampling, especially in the case of free trichome concentrations. Semi-automatic, underwater sampling methods such as those employed by Davis and McGillicuddy (2006) seem to provide an attractive solution, although currently they are unable to record free trichome abundance.

Here, we have found abundances comparable to those found by the VPR, and we have estimated contributions up to 58% to N_2 fixation by free trichomes. Jointly, these make it desirable either to refine semi-automatic samplers or to combine different approaches in future studies. The combination of different methods would allow the simultaneous, independent assessment of the three components of *Trichodesmium* populations. Both net and bottle samples can be further processed in the laboratory to obtain individual size measurements as in this study. In this way,

the systematic changes in size and population structure found here highlighted a potential role for these characteristics in the wide range of N_2 fixation rates reported in the literature (see also Orcutt et al., 2001; Breitbarth et al., 2007; Goebel et al., 2007). This approach, although severely limited because of its exploratory character, was based on well-established ecological principles (e.g. Brown et al., 2004). In this sense, it makes desirable the inclusion of size and temperature in future experiments and measurements involving *Trichodesmium*. This will not only improve our current understanding of N_2 fixation, but it will also set a mechanistic basis to predict the near future of the N cycle in a warmer ocean where *Trichodesmium* distributional range and importance migth increase.

Acknowledgements

We thank the crew and scientific CARPOS team onboard R.V. *Herspérides*, especially L. Blanco Bercial, J. Sostres, and L. Viesca. J. Escánez and J. F. Domínguez (IEO Canarias) kindly provided oxygen and nutrient concentrations; while E. Aguiar and E. Teira (Universidad de Vigo) measured size-fractionated Chl *a* concentrations. T. Westberry (Oregon State University) kindly provided his code and advice on applying the semi-analytic *Trichodesmium* bloom detection algorithm (WSS05). We also thank the NASA Ocean Biology Processing Group at the Goddard Space Flight Center and the Jet Propulsion Laboratory (NASA) for the availability, production and maintenance of MODIS and QuickSCAT data, respectively. The altimeter products were produced by SSALTO/DUACS and distributed by AVISO with support from CNES. Comments by I. Martínez, L. Blanco Bercial, J.L. Acuña, and N.F. Weidberg, and five anonymous referees improved greatly the quality of this paper and are especially acknowledged. We greatly appreciate editorial advice and detailed review by M.E. Bacon. RGG was supported by an undergraduate fellowship from MEC; JH by research contracts from CARPOS (MEC) and RADIAL (IEO-Universidad de Oviedo) projects; and FGT by a FICYT "Severo Ochoa" fellowship (PCTI 2006-09, Gobierno del Principado de Asturias). This research has been supported by project CARPOS (MEC, REN2003-09532-C03-03).

Appendix A

The metabolic theory of ecology argues that biological processes, from respiration and photosynthesis to patterns in trophic dynamics, can be defined by simple relationships given by individual size and temperature scaling (Brown et al., 2004). These parameters have been shown to summarize most of the variation in the performance of any metabolic process. Here, we have take advantage of this and express N_2 fixation rates as any other metabolic rate:

$$I \alpha M^{3/4} e^{-E/kT}, \quad \text{(A1)}$$

where I is the rate of N_2 fixation, M is individual mass, E is activation energy, k=8.62 $\times 10^{-5}$ eV K^{-1} is Boltzmann's constant, and T is absolute temperature, measured in K. The first term on the right side shows the nearly universal scaling of whole-organism metabolic rate as a 0.75 potential of mass. The second term on the right reflects the exponential dependence of biochemical processes on temperature, parameterized using the Boltzmann factor (also called the Van't Hoff-Arrhenius relation).

This model, and some elaborations based on this basic specification, have been tested successfully for a wide series of processes in both the marine and the terrestrial realms (e.g. Brown et al., 2004), although most studies have focused on interspecific allometries (López-Urrutia et al., 2006; O'Connor et al., 2007). Here we used this equation to infer how N_2 fixation rates differed between the different stations. This represents a simple way of comparison between rates derived from abundance and standard conversion factors and those expected when changes in size structure and temperature are taken into account. This approach is obviously flawed for many reasons (e.g. changes in physiological status and carbon content are ignored, and also genotypic differences), although it could be acceptable for exploring the potential impact of systematic changes in *Trichodesmium* size and temperature between stations.

To obtain values proportional to the expected fixation rate, we used trichome volume as a proxy of size and assumed constant element ratios in *Trichodesmium* along the transect. Note also that we conserved the 0.33 equivalence between free trichomes and those forming colonies. We further assumed a constant scaling of 0.75 between N_2 fixation and mass. Absolute temperature values were the same as those presented in Table 1, obtained by Riemann integration of CTD values for the mixed layer. The activation energy was taken from López-Urrutia et al. (2006) and set as a constant with value E=0.33 eV. Using all of these parameters, and based on our measurements on trichome volume and of the number of trichomes forming each kind of colony at each station, we estimated the size- and temperature-corrected contribution of each morphotype to total N_2 fixation, adjusting finally the values to match the total N_2 fixation estimated only from abundance data. We finally explored the influence of temperature and size variation by estimating fixation rates, fixing either temperature or the size of the trichomes of each morphotype to estimated means along the transect.

Appendix B. Supplementary material

Supplementary data associated with this article can be found in the online version at doi:10.1016/j.dsr.2009.09.005.

References

Barton, E.D., Arístegui, J., Tett, P., Cantón, M., García-Braun, J., Hernández-León, S., Nykjaer, L., Almeida, C., Almunia, J., Ballesteros, S., Basterretxea, G., Escánez, J., García-Weill, L., Hernández-Guerra, A., López-Laatzen, F., Molina, R., Montero, M.F., Navarro-Pérez, E., Rodríguez, J.M., van Lenning, K., Vélez, H., Wild, K., 1998. The transition zone of the canary current upwelling region. Prog. Oceanogr. 41, 455–504.

Berman-Frank, I., Cullen, J.T., Shaked, Y., Sherrell, R.M., Falkowski, P.G., 2001. Iron availability, cellular iron quotas, and nitrogen fixation in *Trichodesmium*. Limnol. Oceanogr. 46, 1249–1260.

Bhat, S.R., Verlecar, X.N., 2006. Some enigmatic aspects of the marine cyanobacterial genus, *Trichodesmium*. Curr. Sci. 91, 18–19.

Breitbarth, E., Oschlies, A., LaRoche, J., 2007. Physiological constrains on the global distribution of *Trichodesmium*—effect of temperature on diazotrophy. Biogeoscience 4, 53–61.

Brown, J.H., Gillooly, J.F., Allen, A.P., Savage, V.M., West, G.B., 2004. Toward a metabolic theory of ecology. Ecology 85, 1771–1789.

Capone, D.G., Zehr, J.P., Paerl, H.W., Bergman, B., Carpenter, E.J., 1997. *Trichodesmium*, a globally significant marine cyanobacterium. Science 276, 1221–1229.

Capone, D.G., Burns, J.A., Montoya, J.P., Subramaniam, A., Mahaffey, C., Gunderson, T., Michaels, A.F., Carpenter, E.J., 2005. Nitrogen fixation by *Trichodesmium* spp: an important source of new nitrogen to the tropical and subtropical North Atlantic Ocean. Global Biogeochem. Cycles 19 (GB2024), 17, doi:10.1029/2004GB002331.

Carpenter, E.J., Subramaniam, A., Capone, D.G., 2004. Biomass and primary productivity of the cyanobacterium *Trichodesmium* spp. in the tropical N Atlantic ocean. Deep-Sea Res. Part I Oceanogr. Res. Pap. 51, 173–203.

Chang, J., 2000. Precision of different methods used for estimating the abundance of the nitrogen-fixing marine cyanobacterium, *Trichodesmium* Ehrenberg. J. Exp. Mar. Biol. Ecol. 245, 215–224.

Davis, C.S., McGillicuddy, D.J., 2006. Transatlantic abundance of the N_2-fixing colonial cyanobacterium *Trichodesmium*. Science 312, 1517–1520.

Deutsch, C., Sarmiento, J.L., Sigman, D.M., Gruber, N., Dunne, J.P., 2007. Spatial coupling of nitrogen inputs and losses in the ocean. Nature 445, 163–167.

Falkowski, P.G., 1997. Evolution of the nitrogen cycle and its influence on the biological sequestration of CO_2 in the ocean. Nature 387, 272–275.
Feldman, G.C., McClain, C.R., 2008. Ocean Color Web, MODIS Reprocessing 1.1 and SeaWiFS Reprocessing 5, NASA Goddard Space Flight Center. Ed. by N. Kuring, and S.W. Bailey. Accessed 30 April 2008, 〈http://oceancolor.gsfc.nasa.gov/〉.
Fraser, J.H., 1966. Zooplankton sampling. Nature 211, 915–916.
Gao, Y., Kaufman, Y.J., Tanré, D., Kolber, D., Falkowski, P.G., 2001. Seasonal distributions of aeolian iron fluxes to the global ocean. Geophys. Res. Lett. 28, 29–32.
Goebel, N.L., Edwards, C.A., Church, M.J., Zehr, J.P., 2007. Modeled contributions of three types of diazotrophs to nitrogen fixation at station ALOHA. ISME J. 1, 606–619.
Grasshoff, K., 1983. Determination of oxygen. In: Grasshoff, K., Ehrhardt, M., Kremling, K. (Eds.), Methods of Seawater Analysis second ed. Verlag Chemie, Weinheim, pp. 61–72.
Gruber, N., 2004. The dynamics of the marine nitrogen cycle and its influence on atmospheric CO_2 variations. In: Follows, M.J., Oguz, T. (Eds.), The Ocean Carbon Cycle and Climate NATO ASI Series. Kluwer Academic, Dordrecht, pp. 97–148.
Hood, R.R., Coles, V.J., Capone, D.G., 2004. Modeling the distribution of *Trichodesmium* and nitrogen fixation in the Atlantic Ocean. J. Geophys. Res. 109 (C06006), 25p, doi:10.1029/2002JC001753.
Isern-Fontanet, J., García-Ladona, E., Font, J., 2003. Identification of marine eddies from altimetric maps. J. Atmos. Oceanic Tech. 20, 772–778.
Johnson, J., Stevens, I., 2000. A fine resolution model of the eastern North Atlantic between the Azores, the Canary Islands and the Gibraltar Strait. Deep-Sea Res. Part I Oceanogr. Res. Pap. 47, 875–899.
Karl, D., Michaels, A., Bergman, B., Capone, D., Carpenter, E., Letelier, R., Lipschultz, F., Paerl, H., Sigman, D., Stal, L., 2002. Dinitrogen fixation in the world's oceans. Biogeochemistry 57/58, 47–98.
Käse, R.H., Siedler, G., 1982. Meandering of the subtropical front south-east of the Azores. Nature 300, 245–246.
Klein, B., Siedler, G., 1989. On the origin of the Azores current. J. Geophys. Res. 94, 6159–6168.
Kolber, Z.S., 2006. Getting a better picture of the ocean's nitrogen budget. Science 312, 1479–1480.
Le Traon, P.Y., Nadal, F., Ducet, N., 1998. An improved mapping method of multisatellite altimeter data. J. Atmos. Oceanic Tech. 15, 522–534.
Letelier, R.M., Karl, D., 1996. Role of *Trichodesmium* spp. in the productivity of the subtropical North Pacific Ocean. Mar. Ecol. Prog. Ser. 133, 263–273.
Letelier, R.M., Karl, D., 1998. *Trichodesmium* spp. physiology and nutrient fluxes in the north pacific subtropical gyre. Aquat. Microb. Ecol. 15, 265–276.
Liu, W.T., Xie, X., 2006. Measuring ocean surface wind from space. In: Gower, J. (Ed.), Remote Sensing of the Marine Environment (Manual Remote Sensing, vol. 6 (3rd ed)). American Society for Photogrammetry and Remote Sensing, Bethesda, pp. 149–178.
Longhurst, A., 2007. Ecological Geography of the Sea. Academic Press, London 542 pp.
López-Urrutia, A., San Martín, E., Harris, R.P., Irigoien, X., 2006. Scaling the metabolic balance of the oceans. Proc. Natl. Acad. Sci. USA 103, 8739–8744.
Mahaffey, C., Michaels, A.F., Capone, D.G., 2005. The conundrum of marine N_2 fixation. Am. J. Sci. 305, 546–595.
Mahowald, N.M., Engelstaedter, S., Luo, C., Sealy, A., Artaxo, P., Benitez-Nelson, C., Bonnet, S., Chen, Y., Chuang, P.Y., Cohen, D.D., Dulac, F., Herut, B., Johansen, A.M., Kubilay, N., Losno, R., Maenhaut, W., Paytan, A., Prospero, J.M., Shank, L.M., Siefert, R.L., 2009. Atmospheric iron deposition: global distribution, variability, and human perturbations. Ann. Rev. Mar. Sci. 1, 245–278.
Marañón, E., Pérez, V., Fernández, E., Anadón, R., Bode, A., González, N., Huskin, I., Isla, A., Morán, X.A.G., Mouriño, B., Quevedo, M., Robinson, C., Serret, P., Teira, E., Varela, M.M., Woodward, E.M.S., Zubkov, M.V., 2007. Planktonic carbon budget in the eastern subtropical North Atlantic. Aquat. Microb. Ecol. 48, 261–275.
MathWorks Inc. 2008. MatLab: The Language of Technical Computing. Accessed 30 April 2008, 〈www.mathworks.com〉.
McClain, C.R., Signorini, S.R., Christian, J.R., 2004. Subtropical gyre variability observed by ocean-color satellites. Deep-Sea Res. Part II Top. Stud. Oceanogr. 51, 281–301.
McGillicuddy, D.J., Anderson, L.A., Doney, S.C., Maltrud, M.E., 2003. Eddy-driven sources and sinks of nutrients in the upper ocean: results from a 0.1° resolution model of the North Atlantic. Global Biogeochem. Cycles 17, 1035, doi:10.1029/2002GB001987.
McGillicuddy, D.J., Anderson, L.A., Bates, N.R., Bibby, T., Buesseler, K.O., Carlson, C.A., Davis, C.S., Ewart, C., Falkowski, P.G., Goldthwait, S.A., Hansell, D.A., Jenkins, W.J., Johnson, R., Kosnyrev, V.K., Ledwell, J.R., Li, Q.P., Siegel, D.A., Steinberg, D.K., 2007. Eddy/wind interactions stimulate extraordinary mid-ocean plankton blooms. Science 316, 1021–1025.
Mills, M.M., Ridame, C., Davey, M., LaRoche, J., Geider, R., 2004. Iron and phosphorus co-limit nitrogen fixation in the eastern tropical North Atlantic. Nature 429, 292–294.
Mittelstaedt, E., 1991. The ocean boundary along the northwest African coast: circulation and oceanographic properties at the sea surface. Prog. Oceanogr. 26, 307–355.
Montoya, J.P., Voss, M., Capone, D.G., 2007. Spatial variation in N_2-fixation rate and diazotroph activity in the tropical Atlantic. Biogeoscience 4, 369–376.
Mouriño, B., Fernández, E., Pingree, R., Sinha, B., Escánez, J., de Armas, D., 2005. Constraining effect of mesoscale features on carbon budget of photic layer in the NE subtropical Atlantic. Mar. Ecol. Prog. Ser. 287, 45–52.
Neuer, S., Torres-Padrón, M.E., Gelado-Caballero, M.D., Rueda, M.J., Hernández-Brito, J., Davenport, R., Wefer, G., 2004. Dust deposition pulses to the eastern subtropical North Atlantic gyre: does ocean's biogeochemistry respond?. Global Biogeochem. Cycles 18, GB4020, doi:10.1029/2004GB002228.
O'Connor, M.I., Bruno, J.F., Gaines, S.D., Halpern, B.S., Lester, S.E., Kinlan, B.P., Weiss, J.M., 2007. Temperature control of larval dispersal and the implications for marine ecology, evolution, and conservation. Proc. Natl. Acad. Sci. USA 104, 1266–1271.
O'Neil, J.M., Roman, M.R., 1992. Grazers and associated organisms of *Trichodesmium*. In: Carpenter, E.J., Capone, D.G., Rueter, J.G. (Eds.), Marine Pelagic Cyanobacteria: *Trichodesmium* and other Diazotrophs. Kluwer Academic Publishers, Dordrecht, pp. 61–73.
Ohki, K., Fujita, Y., 1988. Aerobic nitrogenase activity measured as acetylene reduction in the marine non-heterocystous cyanobacterium *Trichodemsium* spp. grown under artificial conditions. Mar. Biol. 98, 111–114.
Orcutt, K.M., Lipschultz, F., Gundersen, K., Arimoto, R., Michaels, A.F., Knap, A.H., Gallon, J.R., 2001. A seasonal study of the significance of N_2 fixation by *Trichodesmium* spp. at the Bermuda Atlantic Time-series Study (BATS) site. Deep-Sea Res. Part II Top. Stud. Oceanogr. 48, 1583–1608.
Oschlies, A., 2002. Nutrient supply to the surface waters of the North Atlantic: a model study. J. Geophys. Res. 107 (C5), 3046, doi:10.1029/2000JC000275.
Oschlies, A., Dietze, H., Kähler, P., 2003. Salt-finger driven enhancement of upper ocean nutrient supply. Geophys. Res. Lett. 30, 2204, doi:10.1029/2003GL018552.
Paerl, H.W., Bebout, B.M., Prufert, L.E., 1989. Bacterial associations with marine *Oscillatoria* sp. (*Trichodesmium* sp.) populations: ecophysiological implications. J. Phycol. 25, 773–784.
Pelegrí, J.L., Marrero-Díaz, A., Ratsimandresey, A.W., 2006. Nutrient irrigation of the North Atlantic. Prog. Oceanogr. 70, 366–406.
Pickard, G.L., Emery, W.J., 1990. Descriptive Physical Oceanography. An Introduction, fifth ed. Butterworth Heinemann, Elsevier, Oxford, UK 320 pp.
Pingree, R.D., 1996. A shallow subtropical subducting westward propagating eddy (swesty). Philos. Trans. R. Soc. Lond. A 354, 979–1026.
Pingree, R.D., García-Soto, C., 2004. Annual westward propagating anomalies near 26°N and eddy generation south of the Canary Islands: remote sensing (altimeter/SeaWiFS) and *in situ* measurements. J. Mar. Biol. Assoc. UK 84, 1105–1115.
R Development Core Team. 2008. *R* 2.7.0.—A language and environment for statistical computing. R Foundation for Statistical Computing, Viena. Accessed 30 May 2008, 〈www.r-project.com〉.
Reynolds, S.E., Mather, R.L., Wolff, G.A., Williams, R.G., Landolfi, A., Sanders, R., Woodward, E.M.S., 2007. How widespread and important is N_2 fixation in the North Atlantic Ocean?. Global Biogeochem. Cycles 21, GB4015, doi:10.1029/2006GB002886.
Saino, T., Hattori, A., 1982. Aerobic nitrogen fixation by the marine non-heterocystous cyanobacterium *Trichodesmium (Oscillatoria)* spp.: its protective mechanism against oxygen. Mar. Biol. 70, 251–254.
Sañudo-Wilhelmy, S.A., Kustka, A.B., Gobler, C.J., Hutchins, D.A., Yang, M., Lwiza, K., Burns, J., Capone, D.G., Raven, J.A., Carpenter, E.J., 2001. Phosphorus limitation of nitrogen fixation by *Trichodesmium* in the central Atlantic Ocean. Nature 411, 66–69.
Sellner, K.G., 1992. Trophodynamics of marine cyanobacteria blooms. In: Carpenter, E.J., Capone, D.G., Rueter, J.G. (Eds.), Marine Pelagic Cyanobacteria: *Trichodesmium* and other Diazotrophs. Kluwer Academic Publishers, Dordrecht, pp. 75–94.
Siedler, G., Onken, R., 1996. Eastern recirculation. In: Krauss, W. (Ed.), The Warmwatersphere of the North Atlantic Ocean. Gebrüder Borntraeger, Berlin, pp. 339–364.
Simó, R., 2001. Production of atmospheric sulfur by oceanic plankton: biogeochemical, ecological and evolutionary links. Trends Ecol. Evol. 16, 287–294.
Sohm, J.A., Capone, D.G., 2006. Phosphorus dynamics of the tropical and subtropical North Atlantic: *Trichodesmium* spp. versus bulk plankton. Mar. Ecol. Prog. Ser. 317, 21–28.
Stramma, L., Siedler, G., 1988. Seasonal changes in the North Atlantic Subtropical Gyre. J. Geophys. Res. 93, 8111–8118.
Tangen, K., 1978. Nets. In: Sournia, A. (Ed.), Phytoplankton Manual. United Nations Educational, Scientific and Cultural Organization, Paris, pp. 50–58.
Tomczak, M., Godfrey, J.S. 2001. Regional Oceanography: An Introduction, second ed. Online edition, 〈http://www.es.flinders.edu.au/~mattom/regoc/pdfversion.html〉.
Tréguer, P., Le Corre, P., 1975. Manuel d'analyse des sels nutritifs dans l'eau de mer (utilisation de l'AutoAnalyzer 'Technicon AII'), second ed. Laboratoire de Chimie Marine, Université de Bretagne Occidentale, Brest 110 pp.
Tyrrell, T., Marañón, E., Poulton, A.J., Bowie, A.R., Harbour, D.S., Woodward, E.M.S., 2003. Large-scale latitudinal distribution of *Trichodesmium* spp. in the Atlantic Ocean. J. Plankton Res. 25, 405–416.
Venables, W.N., Ripley, B.D., 2002. Modern Applied Statistics with *S*, fourth ed. Springer Series on Statistics and Computing, New York 495 pp.
Volpe, G., Banzon, V.F., Evans, R.H., Santoleri, R., Mariano, A.J., Sciarra, R., 2009. Satellite observations of the impact of dust in a low-nutrient, low-chlorophyll region: fertilization or artifact?. Global Biogeochem. Cycles 23, GB3007, doi:10.1019/2008GB003216.
Westberry, T.K., Siegel, D.A., Subramaniam, A., 2005. An improved bio-optical model for the remote sensing of *Trichodesmium* spp. blooms. J. Geophys. Res. 110, C06012, doi:10.1029/2004JC002517.

Westberry, T.K., Siegel, D.A., 2006. Spatial and temporal distribution of *Trichodesmium* blooms in the world's oceans. Global Biogeochem. Cycles 20, GB4016, doi:10.1029/2005GB002673.

Williams, R.G., Follows, M.J., 2003. Physical transport of nutrients and the maintenance of biological production. In: Fasham, M. (Ed.), Ocean Biogeochemistry: The Role of the Ocean Carbon Cycle in Global Change. Springer, New York, pp. 19–51.

Wilson, C., Qiu, X., 2008. Global distribution of summer chlorophyll blooms in the oligotrophic gyres. Prog. Oceanogr. 78, 107–134.

Yentsch, C.S., Menzel, D.W., 1963. A method for the determination of phytoplankton chlorophyll and phaeophytin fluorescence. Deep-Sea Res. 10, 221–231.